

# 3D Covalent Organic Frameworks Selectively Crystallized through Conformational Design

Ha L. Nguyen, Cornelius Gropp, Yanhang Ma, Chenhui Zhu, and Omar M. Yaghi\*



Cite This: *J. Am. Chem. Soc.* 2020, 142, 20335–20339



Read Online

ACCESS |



Metrics & More



Article Recommendations



Supporting Information

**ABSTRACT:** We present a strategy whereby selective formation of imine covalent organic frameworks (COFs) based on linking of triangles and squares into the **fjh** topology was achieved by the conformational design of the building units. 1,3,5-Trimethyl-2,4,6-tris(4-formylphenyl)benzene (TTFB, triangle) and 1,1,2,2-tetrakis(4-aminophenyl)ethene (ETTA, square) were reticulated into [(TTFB)<sub>4</sub>(ETTA)<sub>3</sub>]<sub>imine</sub> termed COF-790, which was fully characterized by spectroscopic, microscopic, and X-ray diffraction techniques. COF-790 exhibits permanent porosity and a Brunauer–Emmett–Teller (BET) surface area of 2650 m<sup>2</sup> g<sup>-1</sup>. Key to the formation of this COF in crystalline form is the pre-designed conformation of the triangle and the square units to give dihedral angles in the range of 75–90°, without which the reaction results in the formation of amorphous product. We demonstrate the versatility of our strategy by also reporting the synthesis and characterization of two isorecticular forms of COF-790, COF-791 and COF-792, based on other square building units.

Covalent organic frameworks (COFs) are two- and three-dimensional (2D and 3D) crystalline structures composed of organic building units linked by covalent bonds.<sup>1–7</sup> Control over the spatial arrangement of the linkers and linkages within the COF backbone has led to frameworks with pre-determined physicochemical properties.<sup>8–11</sup> In the synthesis of crystalline COFs, the geometry and connectivity of the starting building units dictate the choice of structures formed.<sup>12–15</sup> However, combination of building units, such as trigonal-planar (3-c) and square-planar (4-c), still presents great challenges,<sup>7,16–18</sup> because they are expected to produce an array of different high-symmetry topologies: **pto**, **tbo**, **mhq-z**, **fjh**, **iab**, **gee**, and **ffc**. The question becomes how a specific COF topology can be targeted selectively so that the other possibilities are eliminated from forming and thereby complicating the purity and crystallinity of the product. Thus, it is paramount in COF chemistry to develop strategies to design building units that hold sufficient information to selectively target a specific topology and only that topology.

In this report, we show how conformational design<sup>19</sup> of the trigonal linkers has led to the **fjh** topology, heretofore unknown for 3D COFs. Formation of an amorphous phase from linkers lacking such conformational information underlined the importance of such a strategy in selectively targeting specific COFs. We further demonstrate the versatility of our strategy by successful crystallization of isorecticular forms (**fjh**) from similar conformationally designed linkers.

To identify the unique metric information needed for **fjh**, this topology was deconstructed into its trigonal-planar and square-planar building units, as shown in Figure 1a. The dihedral angles between these units are found to be 75–90°. Based on this information, an **fjh** imine-linked framework should result by combining 1,3,5-trimethyl-2,4,6-tris(4-formylphenyl)benzene (TTFB) with 1,1,2,2-tetrakis(4-aminophenyl)ethene (ETTA); see Supporting Information

(SI), section S2). The positions of the methyl groups in TTFB ensure a dihedral angle in the desired range of 75–90°. Accordingly, we synthesized a molecular model system of the TTFB linker and found dihedral angles of 74°, 83°, and 90°, as shown in Figure 1b (see SI, section S3). Encouraged by this structural validation obtained from the model compound, we used the TTFB and ETTA linkers to crystallize [(TTFB)<sub>4</sub>(ETTA)<sub>3</sub>]<sub>imine</sub> (termed COF-790) having the 3D **fjh** topology (Figure 1c). COF-790 was synthesized solvothermally from TTFB and ETTA in a 4:3 molar ratio in nitrobenzene:mesitylene (3:1 volumetric ratio) at 85 °C for 72 h. A modulator, *p*-toluidine (7 equiv), was added (see SI, section S2). COF-790 was isolated, solvent exchanged with *N,N*-dimethylformamide, 0.1 M NH<sub>4</sub>OH in methanol, methanol, and chloroform, and then activated under dynamic vacuum at 90 °C for 4 h to yield the crystalline compound as a yellow powder in 22% yield (see SI, section S2). COF-790 was fully characterized by Fourier transform infrared (FT-IR) and solid- and solution-state nuclear magnetic resonance (NMR) spectroscopies, elemental analysis (EA), thermogravimetric analysis (TGA), scanning electron microscopy (SEM), powder X-ray diffraction (PXRD), nitrogen sorption, and transmission electron microscopy (TEM; see SI, sections S3–S10).

The FT-IR spectroscopic traces of COF-790 indicated imine formation ( $\nu_{C=N} = 1628 \text{ cm}^{-1}$ ), with no identifiable aldehyde stretches ( $\nu_{C=O} = 1692 \text{ cm}^{-1}$ ) remaining (see SI, section S4). Complete imine formation of COF-790 was corroborated by

Received: October 20, 2020

Published: November 13, 2020



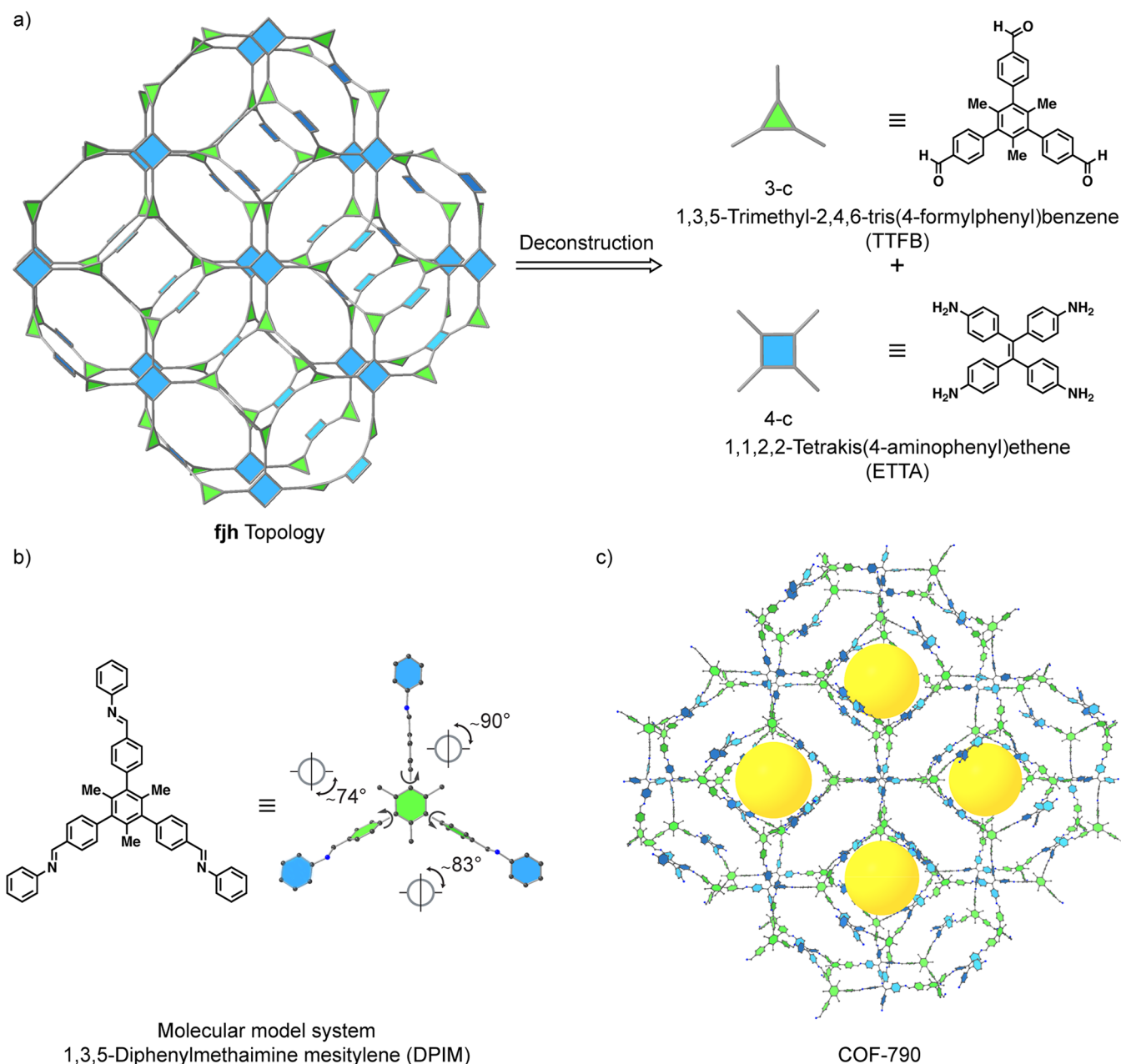


**Figure 1.** Synthesis of a 3D COF of the **fjh** topology through conformational linker design. (a) The **fjh** deconstructs into 3-c and 4-c building units and their corresponding chemical equivalents: 1,3,5-trimethyl-2,4,6-tris(4-formylphenyl)benzene (TTFB) and 1,1,2,2-tetrakis(4-aminophenyl)ethene (ETTA), respectively. (b) Single-crystal X-ray structure of the trigonal-planar molecular model system with dihedral angles of 74–90° and (c) crystal structure of  $[(\text{TTFB})_4(\text{ETTA})_3]_{\text{imine}}$  termed COF-790, with yellow spheres placed inside the pores at the van der Waals radii of the framework atoms.

$^{13}\text{C}$  cross-polarization magic angle spinning (CP-MAS) NMR spectroscopy, displaying characteristic  $\text{C}=\text{N}$  resonances at 161.7 ppm and the absence of resonances corresponding to aldehyde groups of the starting material TTFB. The resonances of the methyl groups located at the center phenyl of the TTFB unit appeared at 18.9 ppm (see SI, section S5).

The atomic composition of COF-790 was determined by EA and found to be  $\text{C}_{198}\text{H}_{144}\text{N}_{12}$ , corresponding to  $[(\text{TTFB})_4(\text{ETTA})_3]_{\text{imine}}$  (Calcd for C, 88.36; H, 5.39; N, 6.25%. Found: C, 83.36; H, 5.65; N, 6.45%; see SI, section S2). The difference in elemental composition between the calculated and the experimental values likely originates from remaining water molecules in the framework (ca. 5.7%), evidence of which was

substantiated by FT-IR spectroscopy and TGA traces. TGA done under a  $\text{N}_2$  atmosphere showed a weight loss of ~5% at 250 °C and an onset in thermal decomposition of COF-790 at around 400 °C (see SI, section S6). The constitution of COF-790 was supported by solution-state NMR of its acid-digested form and demonstrated a 4:3 ratio of TTFB:ETTA (Figure 2a). This result was consistent with the FT-IR and CP-MAS  $^{13}\text{C}$  NMR results, pointing to negligible defects within the crystallites and the absence of unreacted aldehyde and amine functionalities of the starting building units TTFB and ETTA (see SI, section S5).

SEM micrographs of the COF-790 crystallites showed a single morphological phase with a homogeneous distribution

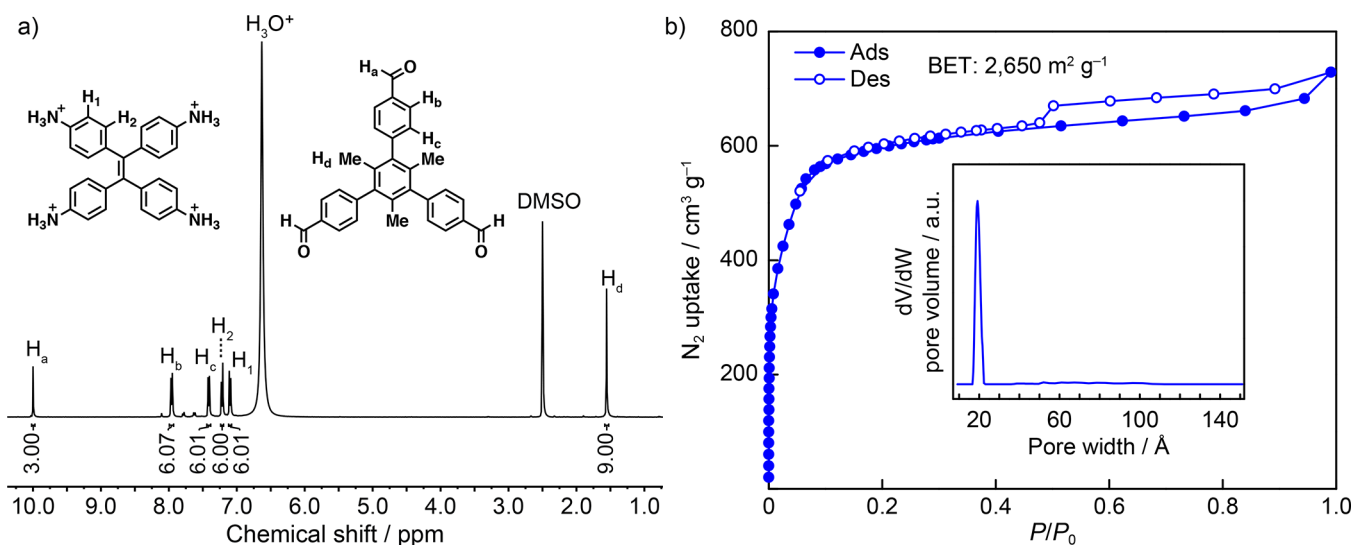


**Figure 2.** Structural and molecular characterization of COF-790. (a) Solution-state NMR spectroscopy of the acid-digested COF-790 indicates a 4:3 stoichiometric ratio of the TTFB:ETTA linkers. (b)  $N_2$  adsorption isotherm at 77 K of COF-790 demonstrates a mesoporous structure with a pore diameter of 20.0 Å and a BET surface area of 2650  $m^2 g^{-1}$ .

of needle-shaped crystals of  $\sim 200$  nm and aggregated spherical particles (SI, section S7). PXRD analysis of the microcrystalline powder of COF-790 confirmed its crystallinity and revealed no diffraction peaks that could be attributed to residual starting materials or reaction additives (Figure 3; see SI, section S8).

The crystal structure was obtained by comparison of the experimental wide-angle X-ray scattering (WAXS) pattern of COF-790 with the simulated PXRD patterns of the model structures. The experimental diffraction pattern of COF-790 matched well with the simulated pattern obtained from the *fh* net, displaying two characteristic peaks at 1.91 and 2.30° ( $\lambda = 1.24$  Å), where the first peak can be indexed as the 110 reflection and the subsequent ones as the 200 and 020 reflections. Importantly, alternative structural models of the *pto*, *tbo*, *mhq-z*, *iab*, *ffc*, and *gee* topologies matched poorly with the experimental results (see SI, section S8).

Additionally, the structural model generated from the *fh* topology displayed one discrete pore size of 21.5 Å (see SI, section S8). To validate our structural model, we measured the  $N_2$  sorption isotherm at 77 K. The  $N_2$  adsorption of COF-790 demonstrated permanent porosity with a mesoporous pore structure and a Type I behavior. The Brunauer–Emmett–Teller (BET) surface area was calculated to be 2650  $m^2 g^{-1}$ . The pore size distribution, estimated from the  $N_2$  isotherm and calculated by density functional theory (DFT) using the cylinder geometry and  $N_2$ -cylindrical pores–oxide surface model, indicated a pore diameter of 20.0 Å (Figure 2b; see SI, section S9). This finding was in good agreement with our structural model (21.5 Å).

Based on these experimental results, a structural model was built, and the crystal structure of COF-790 was assigned to the space group *Iba2* (No. 45) with unit cell parameters of  $a = 62.56$  Å,  $b = 60.32$  Å, and  $c = 30.06$  Å. Structural details are given in the SI, section S8. High-resolution TEM (HRTEM; see SI, section S10) showed two kinds of lattice  $d$ -spacings of 20 and 28 Å, corresponding to the lattice planes of 121/211 and 020.

Under synthetic conditions comparable to those used for the synthesis of COF-790, but with the TFB lacking the methyl

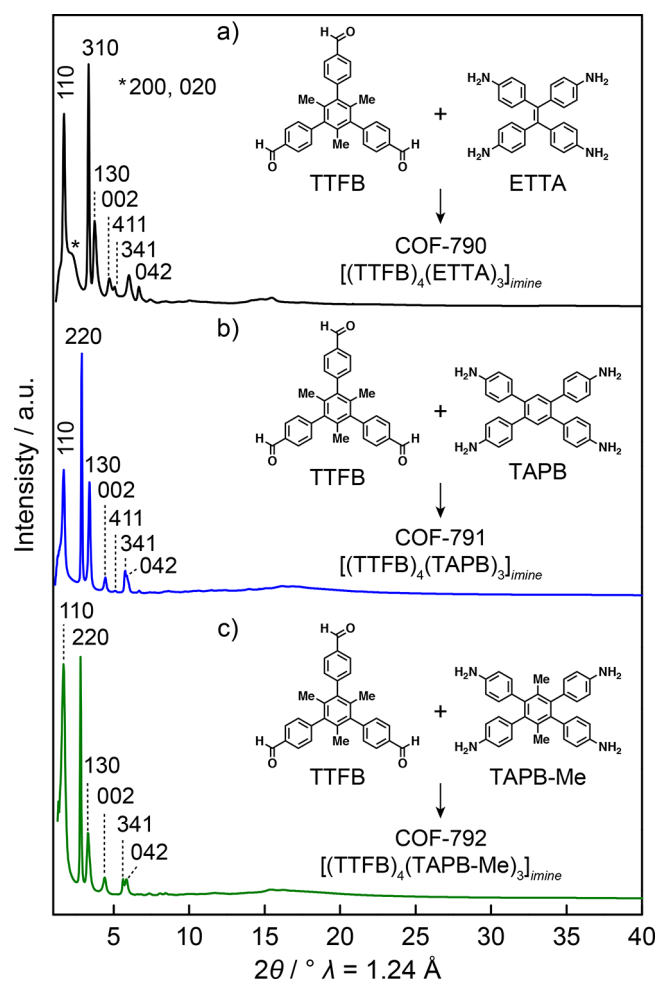


**Figure 3.** WAXS patterns of COF-790 (a), COF-791 (b), and COF-792 (c), indicating a shift of the lowest angle peak to lower  $2\theta$  values with increasing length of the 4-c linker from COF-790 to COF-791 and COF-792.

groups and therefore the conformational information, we obtained an amorphous solid (see SI, section S8). We

attributed this to the formation of multiple phases, preventing selective crystallization of **fjh**. Alternative synthetic conditions favor the formation of a 2D COF with a defected **ttt** topology.<sup>21</sup> In this 2D COF, the TFB units adopt dihedral angles between 32 and 51°.

To demonstrate the versatility of our design strategy, we also report a series of isorecticular structures of COF-790, namely COF-791 and COF-792, where we replaced the square-planar ETTA unit of COF-790 with 1,2,4,5-tetrakis(4-aminophenyl)benzene (TAPB) and 1,2,4,5-tetrakis(4-aminophenyl)-3',6'-dimethylbenzene (TAPB-Me), respectively (Figure 3). COF-791 ( $[(\text{TTFB})_4(\text{TAPB})_3]_{\text{imine}}$ ) and COF-792 ( $[(\text{TTFB})_4(\text{TAPB-Me})_3]_{\text{imine}}$ ) were synthesized and characterized as demonstrated for COF-790 (see SI, section S2). Formation of COF-791 and COF-792 was corroborated by FT-IR and CP-MAS <sup>13</sup>C NMR spectroscopies. Disappearance of the aldehyde functionality, assigned to the resonances at  $\nu_{\text{C=O}} = 1692 \text{ cm}^{-1}$ , indicated successful imine formation ( $\nu_{\text{C=N}} = 1628 \text{ cm}^{-1}$ ; see SI, section S4). Solid-state <sup>13</sup>C NMR spectra of COF-791 and COF-792 displayed resonances associated with the imine functionality at 161.5 and 160.6 ppm, respectively. Moreover, at 18.7 and 18.9 ppm, we observed the resonances corresponding to the methyl groups in COF-791 and COF-792 (see SI, section S5).

The atomic compositions of COF-791 and COF-792 were determined by EA (COF-791: Calcd for  $\text{C}_{210}\text{H}_{150}\text{N}_{12}$  corresponding to  $[(\text{TTFB})_4(\text{TAPB})_3]_{\text{imine}}$ : C, 88.76; H, 5.32; N, 5.92%. Found: C, 86.80; H, 5.51; N, 5.97%. COF-792: Calcd for  $\text{C}_{216}\text{H}_{162}\text{N}_{12}$  corresponding to  $[(\text{TTFB})_4(\text{TAPB-Me})_3]_{\text{imine}}$ : C, 88.67; H, 5.58; N, 5.75%. Found: C, 86.58; H, 6.02; N, 5.55%). COF-791 and -792 showed an onset in thermal decomposition under a N<sub>2</sub> atmosphere at around 400 °C (see SI, section S6). SEM micrographs indicated a homogeneous size in crystallites of cube (~300–400 nm) and needle shapes (~200 nm) for COF-791 and -792, respectively.

The crystal structures of COF-791 and -792 were built analogously to the **fjh** net of COF-790. Based on the model structures, COF-791 and COF-792 displayed pore diameters of 22.8 and 22.4 Å, respectively. N<sub>2</sub> adsorption isotherms at 77 K of COF-791 and COF-792 demonstrated permanent porosity and a Type I isotherm with mesoporous pore structures. The BET surface area was calculated to be 1920 m<sup>2</sup> g<sup>-1</sup> for COF-791 and 2250 m<sup>2</sup> g<sup>-1</sup> for COF-792. Analysis of the pore size distribution yielded diameters of 19.0 Å for COF-791 and 22.6 Å for COF-792, both in good agreement with their theoretical values estimated from their model structures.

The lowest angle peaks of COF-791 and -792, as measured by WAXS, appeared at 1.89° ( $\lambda = 1.24 \text{ \AA}$ ). A shift to lower *d*-spacing was observed for the isorecticular forms of COF-790 due to the slight enlargement of the unit cell parameters with increasing linker lengths of the TAPB units (Figure 3). HRTEM analysis of COF-791 indicated lattice fringes of 25 Å, which were attributed to the 220 lattice plane. Owing to the higher relative crystallinity of COF-792, lattice fringes with *d*-spacings of 44 Å were identified, which corresponds to the 110 lattice plane (see SI, Section S10).

## ■ ASSOCIATED CONTENT

### Supporting Information

The Supporting Information is available free of charge at <https://pubs.acs.org/doi/10.1021/jacs.0c11064>.

Synthesis and full characterization of COF-790, COF-791, and COF-792 including EA, FT-IR spectroscopy, NMR spectra, PXRD data, computational modeling, gas uptake measurements, TGA, SEM images, and HRTEM images (PDF)

X-ray crystallographic data for COF-790 (CIF)

X-ray crystallographic data for COF-791 (CIF)

X-ray crystallographic data for COF-792 (CIF)

X-ray crystallographic data for TAPB-Amine (CIF)

X-ray crystallographic data for TTFP-Aniline (CIF)

## ■ AUTHOR INFORMATION

### Corresponding Author

Omar M. Yaghi – Department of Chemistry, University of California Berkeley; Kavli Energy Nanoscience Institute at UC Berkeley; and Berkeley Global Science Institute, Berkeley, California 94720, United States; Joint UAEU-UC Berkeley Laboratories for Materials Innovations, UAE University, Al-Ain, United Arab Emirates; [orcid.org/0000-0002-5611-3325](https://orcid.org/0000-0002-5611-3325); Email: [yaghi@berkeley.edu](mailto:yaghi@berkeley.edu)

### Authors

Ha L. Nguyen – Department of Chemistry, University of California Berkeley; Kavli Energy Nanoscience Institute at UC Berkeley; and Berkeley Global Science Institute, Berkeley, California 94720, United States; Joint UAEU-UC Berkeley Laboratories for Materials Innovations, UAE University, Al-Ain, United Arab Emirates; [orcid.org/0000-0002-4977-925X](https://orcid.org/0000-0002-4977-925X)

Cornelius Gropp – Department of Chemistry, University of California Berkeley; Kavli Energy Nanoscience Institute at UC Berkeley; and Berkeley Global Science Institute, Berkeley, California 94720, United States; [orcid.org/0000-0002-5843-8158](https://orcid.org/0000-0002-5843-8158)

Yanhang Ma – School of Physical Science and Technology, ShanghaiTech University, Shanghai 201210, China; [orcid.org/0000-0003-4814-3740](https://orcid.org/0000-0003-4814-3740)

Chenhui Zhu – Advanced Light Source, Lawrence Berkeley National Laboratory, Berkeley, California 94720, United States

Complete contact information is available at: <https://pubs.acs.org/10.1021/jacs.0c11064>

### Notes

The authors declare no competing financial interest.

## ■ ACKNOWLEDGMENTS

C.G. is a Leopoldina postdoctoral fellow of the German National Academy of Science (LPDS 2019-02) and acknowledges the receipt of a fellowship of the Swiss National Science Foundation (P2EZP2-184380). We acknowledge King Abdulaziz City for Science and Technology as part of a joint KACST–UC Berkeley collaboration and UAE University as part of a joint UAEU–UC Berkeley collaboration. We thank Mr. Hao Lyu (Yaghi group, UC Berkeley) for help in obtaining SEM images and Dr. Tianqiong Ma (Yaghi group, UC Berkeley) for initial efforts in growing crystals of COF-791. This research used beamline 7.3.3 of the Advanced Light Source, which is a DOE Office of Science User Facility under contract no. DE-AC02-05CH11231. This work is supported by the National Natural Science Foundation of China (No. 21875140) and C<sub>h</sub>EM SPST, ShanghaiTech University

(#EM02161943) for TEM measurements. We acknowledge the College of Chemistry Nuclear Magnetic Resonance Facility for resources—instruments are partially supported by NIH S10OD024998—and staff assistance from Dr. Hasan Celik and Dr. Wei-Chih Liao.

## REFERENCES

- (1) Yaghi, O. M.; Kalmutzki, M. J.; Diercks, C. S. *Introduction to Reticular Chemistry: Metal-organic frameworks and covalent organic frameworks*; Wiley-VCH: Weinheim, 2019; p 509.
- (2) Cote, A. P.; Benin, A. I.; Ockwig, N. W.; O’Keeffe, M.; Matzger, A. J.; Yaghi, O. M. Porous, crystalline, covalent organic frameworks. *Science* **2005**, *310*, 1166–1170.
- (3) El-Kaderi, H. M.; Hunt, J. R.; Mendoza-Cortés, J. L.; Côté, A. P.; Taylor, R. E.; O’Keeffe, M.; Yaghi, O. M. Designed synthesis of 3D covalent organic frameworks. *Science* **2007**, *316*, 268–272.
- (4) Feng, X.; Ding, X.; Jiang, D. Covalent Organic Frameworks. *Chem. Soc. Rev.* **2012**, *41*, 6010–6022.
- (5) Diercks, C. S.; Yaghi, O. M. The Atom, the Molecule, and the Covalent Organic Framework. *Science* **2017**, *355*, No. eaal1585.
- (6) Kandambeth, S.; Dey, K.; Banerjee, R. Covalent Organic Frameworks: Chemistry beyond the Structure. *J. Am. Chem. Soc.* **2019**, *141*, 1807–1822.
- (7) Guan, X.; Chen, F.; Fang, Q.; Qiu, S. Design and Applications of Three Dimensional Covalent Organic Frameworks. *Chem. Soc. Rev.* **2020**, *49*, 1357–1384.
- (8) Jiang, J.; Zhao, Y.; Yaghi, O. M. Covalent Chemistry beyond Molecules. *J. Am. Chem. Soc.* **2016**, *138*, 3255–3265.
- (9) Lohse, M. S.; Bein, T. Covalent Organic Frameworks: Structures, Synthesis, and Applications. *Adv. Funct. Mater.* **2018**, *28*, 1705553.
- (10) Song, Y.; Sun, Q.; Aguila, B.; Ma, S. Opportunities of Covalent Organic Frameworks for Advanced Applications. *Adv. Sci.* **2019**, *6*, 1801410.
- (11) Li, Z.; He, T.; Gong, Y.; Jiang, D. Covalent Organic Frameworks: Pore Design and Interface Engineering. *Acc. Chem. Res.* **2020**, *53*, 1672–1685.
- (12) Ding, S. Y.; Wang, W. Covalent Organic Frameworks (COFs): From Design to Applications. *Chem. Soc. Rev.* **2013**, *42*, 548–568.
- (13) Gao, C.; Li, J.; Yin, S.; Sun, J.; Wang, C. Twist Building Blocks from Planar to Tetrahedral for the Synthesis of Covalent Organic Frameworks. *J. Am. Chem. Soc.* **2020**, *142*, 3718–3723.
- (14) Zhu, Q.; Wang, X.; Clowes, R.; Cui, P.; Chen, L.; Little, M. A.; Cooper, A. I. 3D Cage COFs: A Dynamic Three-Dimensional Covalent Organic Framework with High-Connectivity Organic Cage Nodes. *J. Am. Chem. Soc.* **2020**, *142*, 16842–16848.
- (15) Gropp, C.; Ma, T.; Hanikel, N.; Yaghi, O. M. Design of Higher Valency in Covalent Organic Frameworks. *Science* **2020**, *370*, No. eabd6406.
- (16) Ma, X.; Scott, T. F. Approaches and Challenges in the Synthesis of Three-Dimensional Covalent-Organic Frameworks. *Commun. Chem.* **2018**, *1*, 98.
- (17) Lan, Y.; Han, X.; Tong, M.; Huang, H.; Yang, Q.; Liu, D.; Zhao, X.; Zhong, C. Materials Genomics Methods for High-Throughput Construction of COFs and Targeted Synthesis. *Nat. Commun.* **2018**, *9*, 5274.
- (18) Kang, X.; Han, X.; Yuan, C.; Cheng, C.; Liu, Y.; Cui, Y. Reticular Synthesis of the Topology Covalent Organic Frameworks. *J. Am. Chem. Soc.* **2020**, *142*, 16346–16356.
- (19) Eddaoudi, M.; Kim, J.; O’Keeffe, M.; Yaghi, O. M.  $\text{Cu}_2[\text{o-Br-C}_6\text{H}_3(\text{CO}_2)_2]_2(\text{H}_2\text{O})_2 \cdot (\text{DMF})_8(\text{H}_2\text{O})_2$ : A Framework Deliberately Designed To Have the NbO Structure Type. *J. Am. Chem. Soc.* **2002**, *124*, 376–377.
- (20) Lu, W.; Yuan, D.; Makal, T. A.; Li, J.-R.; Zhou, H.-C. A Highly Porous and Robust (3,3,4)-Connected Metal-Organic Framework Assembled with a 90° Bridging-Angle Embedded Octacarboxylate Ligand. *Angew. Chem., Int. Ed.* **2012**, *51*, 1580–1584.
- (21) Zhang, B.; Mao, H.; Matheu, R.; Reimer, J. A.; Alshimiri, S. A.; Alshihri, S.; Yaghi, O. M. Reticular synthesis of multinary covalent organic frameworks. *J. Am. Chem. Soc.* **2019**, *141*, 11420–11424.